

Progress Towards a No-Lose Theorem for NMSSM Higgs Discovery at the LHC and LC Complementarity

Jack Gunion

Davis Institute for High Energy Physics, U.C. Davis

Collaborators: U. Ellwanger, C. Hugonie, S. Moretti

Les Houches, LHC/LC Workshop, 2003

Outline

- Introduction
- The parameter space
- The Inputs and Scan Procedure
- The No-Higgs-to-Higgs Decay Part of Parameter Space
- The Full Parameter Space
- LHC/LC Complementarity
- Conclusions

Introduction

- One of the key ingredients in the no-lose theorem for MSSM Higgs boson discovery is the fact that the SM-like Higgs boson (the h when $m_A \gtrsim 125$ GeV or H when $m_A \lesssim 115$ GeV) never has significant decays to other Higgs bosons ($h \rightarrow AA$ or $H \rightarrow AA, hh$, respectively). In the NMSSM, Higgs boson masses are not very strongly correlated, and $h_1 \rightarrow a_1 a_1$ or $h_2 \rightarrow a_1 a_1$ decays can be prominent. Such decays fall outside the scope of the usual detection modes for the SM-like MSSM h on which the MSSM no-lose LHC theorem largely relies.

The question: does this make an absolute LHC no-lose theorem for the NMSSM impossible.

- In earlier work (last LHC/LC workshop), a partial no-lose theorem for NMSSM Higgs boson discovery at the LHC was established.

In particular, it was shown that the LHC would be able to detect at least one of the NMSSM Higgs bosons (typically, one of the lighter CP-even Higgs states) throughout the full parameter space of the model,

excluding only those parameter choices for which there is sensitivity to the model-dependent decays of Higgs bosons to other Higgs bosons and/or superparticles.

- Here, we will retain the assumption of a heavy superparticle spectrum and address the question of whether or not this no-lose theorem can be extended to those regions of NMSSM parameter space for which Higgs bosons can decay to other Higgs bosons.

We find that the parameter choices such that the “standard” discovery modes fail are such that there is a SM-like Higgs boson h that mainly decays to aa . (When used generically, the symbol h will now refer to $h = h_1, h_2$ or h_3 and the symbol a will refer to $a = a_1$ or a_2). Detection of $h \rightarrow aa$ will be difficult since each a will decay primarily to either $b\bar{b}$ (or 2 jets if $m_a < 2m_b$) and $\tau^+\tau^-$, yielding final states that will typically have large backgrounds at the LHC.

- In the end, we find a signal at the LHC even for this most difficult case, but it will be hard to be sure it is a Higgs boson.

The parameter space

- We consider the simplest version of the NMSSM, where the term $\mu\widehat{H}_1\widehat{H}_2$ in the superpotential of the MSSM is replaced by (we use the notation \widehat{A} for the superfield and A for its scalar component field)

$$\lambda\widehat{H}_1\widehat{H}_2\widehat{S} + \frac{\kappa}{3}\widehat{S}^3, \quad (1)$$

so that the superpotential is scale invariant.

- We make no assumption on “universal” soft terms. Hence, the five soft supersymmetry breaking terms

$$m_{H_1}^2 H_1^2 + m_{H_2}^2 H_2^2 + m_S^2 S^2 + \lambda A_\lambda H_1 H_2 S + \frac{\kappa}{3} A_\kappa S^3 \quad (2)$$

are considered as independent.

- The masses and/or couplings of sparticles are assumed to be such that their contributions to the loop diagrams for $gg \rightarrow h$ and $\gamma\gamma \rightarrow h$ couplings are negligible.
- In the stop sector, which appears in the radiative corrections to the Higgs potential, we chose the soft masses $m_Q = m_T \equiv M_{susy} = 1 \text{ TeV}$.
- We also scan over the stop mixing parameter, related to M_{susy} and the soft mixing parameter A_t by $X_t \equiv 2 \frac{A_t^2}{M_{susy}^2 + m_t^2} \left(1 - \frac{A_t^2}{12(M_{susy}^2 + m_t^2)} \right)$. As in the MSSM, the value $X_t = \sqrt{6}$ – so called maximal mixing – maximizes the radiative corrections to the Higgs boson masses, and we found that it leads to the most challenging points in NMSSM parameter space.
- We adopt the convention $\lambda, \kappa > 0$, in which $\tan\beta$ can have either sign. We require $|\mu_{\text{eff}}| = \lambda\langle S \rangle > 100 \text{ GeV}$; otherwise a light chargino would have been detected at LEP.

Inputs and Scanning Procedure

- We have performed a numerical scan over the free parameters.

For each point, we computed the masses and mixings of the CP-even and CP-odd Higgs bosons, h_i ($i = 1, 2, 3$) and a_j ($j = 1, 2$), taking into account radiative corrections up to the dominant two loop terms.

We eliminated parameter choices excluded by LEP constraints on $e^+e^- \rightarrow Zh_i$ and $e^+e^- \rightarrow h_i a_j$. The latter provides an upper bound on the $Zh_i a_j$ reduced coupling, R'_{ij} , as a function of $m_{h_i} + m_{a_j}$ for $m_{h_i} \simeq m_{a_j}$.

Finally, we calculated m_{h^\pm} and required $m_{h^\pm} > 155$ GeV, so that $t \rightarrow h^\pm b$ would not be seen.

- LHC discovery modes for a Higgs boson considered were (with $\ell = e, \mu$):
 - 1) $gg \rightarrow h/a \rightarrow \gamma\gamma$;
 - 2) associated Wh/a or $t\bar{t}h/a$ production with $\gamma\gamma\ell^\pm$ in the final state;
 - 3) associated $t\bar{t}h/a$ production with $h/a \rightarrow b\bar{b}$;
 - 4) associated $b\bar{b}h/a$ production with $h/a \rightarrow \tau^+\tau^-$;
 - 5) $gg \rightarrow h \rightarrow ZZ^{(*)} \rightarrow 4$ leptons;
 - 6) $gg \rightarrow h \rightarrow WW^{(*)} \rightarrow \ell^+\ell^-\nu\bar{\nu}$;
 - 7) $WW \rightarrow h \rightarrow \tau^+\tau^-$;
 - 8) $WW \rightarrow h \rightarrow WW^{(*)}$.
- We estimated the expected statistical significances at the LHC in all Higgs boson detection modes 1) – 8) by rescaling results for the SM Higgs boson and/or the the MSSM h, H and/or A .

The rescaling factors are determined by R_i (also called $CV(i)$), t_i (also called $Ct(i)$) and $b_i = \tau_i$ (also called $Cb(i)$), the ratios of the VVh_i , $t\bar{t}h_i$ and $b\bar{b}h_i, \tau^+\tau^-h_i$ couplings, respectively, to those of a SM Higgs boson.

Of course $|R_i| < 1$, but t_i and b_i can be larger, smaller or even differ in sign with respect to the SM.

For the CP-odd Higgs bosons, $R'_i = 0$ at tree-level; t'_j and b'_j are the ratios of the $i\gamma_5$ couplings for $t\bar{t}$ and $b\bar{b}$, respectively, relative to SM-like strength.

- For each Higgs state, we calculated all branching ratios, including those for modes $i) - viii)$ listed later, using an adapted version of the FORTRAN code HDECAY.
- At the moment, the $N_{SD} = S/\sqrt{B}$ values employed are those indicated by ** in the attached tables of all LHC simulation results of which we are aware. Note that the $t\bar{t}h \rightarrow t\bar{t}b\bar{b}$ mode will be quite important. We have had the experimentalists extrapolate this beyond the usual SM mass range of interest. The ** results employed for this channel are quoted for $B(h \rightarrow b\bar{b}) = 1$.

At the moment we are uniformly employing $K_S = K_B = 1$ results, awaiting the time when all K factors are known.

For all cases where both K_S and K_B are known, their inclusion improves the N_{SD} value.

- Some things that have changed recently:

1. The $gg \rightarrow h_{\text{SM}} \rightarrow \gamma\gamma$ N_{SD} values from CMS have gotten smaller (detector cracks ...).
2. The CMS $t\bar{t}h_{\text{SM}} \rightarrow t\bar{t}b\bar{b}$ N_{SD} values are *much* larger than the ATLAS values.
3. The experimental evaluations of the WW fusion channels yield lower N_{SD} values than the original theoretical estimates.

- For each mode, our procedure has been to use the results for the “best detector” (e.g. CMS for the $t\bar{t}h$ channel), assuming $L = 300\text{fb}^{-1}$ for that *one* detector.

Table 1: $gg \rightarrow h \rightarrow \gamma\gamma$

m [GeV]	70	80	90	100	110	120	130	140	150
S/\sqrt{B} (CMS TP, LHCC 94-38, fig. 12.5)	-	4.3	6.5	8.5	10.5	12.2	12.8	10.4	8.1
S/\sqrt{B} (CMS Note 1997/057, fig. 1)	2.7	5.0	6.6	8.5	11.3	12.9	12.2	10.0	7.3
S/\sqrt{B} (Lassila-Perini Thesis, p. 126, with $K_s, K_b \neq 1$)	-	-	-	6.3	8.7	10.3	10.4	9.7	7.1
S/\sqrt{B} (Lassila-Perini Thesis, p. 126, with $K_s, K_b \neq 1, gg$ only)	-	-	-	5.3	7.3	8.6	8.6	8.0	5.8
S/\sqrt{B} (hep-ph/0002036, tab. 1 = L.-P. no K?)	-	-	-	5.1	7.0	8.1	8.9	8.4	6.3
S/\sqrt{B} (CMS 100 fb ⁻¹ , $K_s = K_b = 1$ [1]) **	-	-	-	5.0	7.0	8.2	10.0	8.5	6.3
S/\sqrt{B} (CMS 100 fb ⁻¹ , $K_s = K_b = 1, gg$ only [2])	-	-	-	4.2	6.0	6.8	8.2	7.0	5.2
S/\sqrt{B} (CMS 30 fb ⁻¹ [4])	-	-	-	3.3	4.4	5.4	5.6	5.4	4.2
S/\sqrt{B} (ATLAS 100 fb ⁻¹ [5])	Already combined with $Wh/t\bar{t}h \rightarrow \gamma\gamma l$								
S/\sqrt{B} (ATLAS 30 fb ⁻¹ [5])	-	1.5	1.9	2.7	3.4	3.9	4.0	3.4	2.6

Table 2: $Wh/t\bar{t}h \rightarrow \gamma\gamma l$

m [GeV]	70	80	90	100	110	120	130	140	150	160	170
S/\sqrt{B} (CMS TP, LHCC 94-38, tab. 12.3)	-	8.8	9.8	11.4	12.1	11.7	-	-	-	-	-
S/\sqrt{B} (CMS Note 1997/057, fig. 1) **	7.8	11	12.9	14.6	14.8	14.5	12.2	10	7.2	5	2.6
S/\sqrt{B} (CMS 100 fb ⁻¹ [4])	-	9.4	10.6	10.9	14.8	15.7	13.2	10.4	8.2	-	-
S/\sqrt{B} (CMS 30 fb ⁻¹ [4])	-	4.2	4.7	4.6	4.9	4.7	-	-	-	-	-

Table 3: $t\bar{t}h \rightarrow t\bar{t}b\bar{b}$

m [GeV]	80	85	90	95	100	105	110	115
S/\sqrt{B} (Sapinski, Les Houches, $BR(h \rightarrow bb) = 1$)	9.6	9.0	8.5	8.2	7.8	7.2	6.7	6.3
S/\sqrt{B} (Sapinski, Acta. Phys. Pol. B30)	8.3	-	-	-	6.5	-	-	-
S/\sqrt{B} (ATLAS 100 fb ⁻¹)	9.5	-	-	-	7.4	-	-	-
S/\sqrt{B} (ATLAS 30 fb ⁻¹)	6.7	-	-	-	5.0	-	-	-
S/\sqrt{B} (CMS Note 2001-054 @ 100 fb ⁻¹ Kb=1.9, Ks=1[3])	11.1	-	8.8	-	8.2	-	6.8	6.3
S/\sqrt{B} (CMS Note 2001-054 @ 100 fb ⁻¹ Kb=1.9, Ks=1.5)	16.6	-	13.1	-	12.3	-	10.2	9.7
S/\sqrt{B} (CMS Note 2001-054 @ 100 fb ⁻¹ no K)	15.3	-	12.1	-	11.3	-	9.4	9.0
S/\sqrt{B} (CMS Note 2001-054 @ 100 fb ⁻¹ no K, $BR(h \rightarrow bb) = 1$ [6]) **	17.9	-	15.0	-	14.1	-	12.3	-
S/\sqrt{B} (CMS 100 fb ⁻¹ [4])	Already combined with $Wh \rightarrow Wb\bar{b}$							
S/\sqrt{B} (CMS 30 fb ⁻¹ [4])	-	-	-	-	4.5	-	3.7	-
m [GeV]	120	125	130	135	140	145	150	
S/\sqrt{B} (Sapinski, Les Houches, $BR(h \rightarrow bb) = 1$)	5.7	4.5	3.6	3.2	2.9	2.5	2.0	
S/\sqrt{B} (Sapinski, Acta. Phys. Pol. B30)	4.0	-	-	-	-	-	-	
S/\sqrt{B} (ATLAS 100 fb ⁻¹)	5.0	-	-	-	-	-	-	
S/\sqrt{B} (ATLAS 30 fb ⁻¹)	3.5	-	-	-	-	-	-	
S/\sqrt{B} (CMS Note 2001-054 @ 100 fb ⁻¹ Kb=1.9, Ks=1)	6.2	-	5.1	-	2.7	-	1.3	
S/\sqrt{B} (CMS Note 2001-054 @ 100 fb ⁻¹ Kb=1.9, Ks=1.5)	9.3	-	7.6	-	4.0	-	1.9	
S/\sqrt{B} (CMS Note 2001-054 @ 100 fb ⁻¹ no K)	8.5	-	7.0	-	3.7	-	1.8	
S/\sqrt{B} (CMS Note 2001-054 @ 100 fb ⁻¹ no K, $BR(h \rightarrow bb) = 1$ [6]) **	12.7	-	13.7	-	11.3	-	10.6	
S/\sqrt{B} (CMS 100 fb ⁻¹ [4])								
S/\sqrt{B} (CMS 30 fb ⁻¹ [4])	3.4	-	2.8	-	-	-	-	

Table 4: $b\bar{b}h/a \rightarrow \tau\bar{\tau}$ at $\tan\beta = 1$

m [GeV]	100	110	120	130	140	150	200
S/\sqrt{B} (ATLAS TDR, fig. 19.62) ($\times 10^2$)	3.9	-	4.6	-	-	4.6	2.9
S/\sqrt{B} (ATLAS TDR, tab. 19.35/36) ($\times 10^2$)	-	-	-	-	-	5.4	-
S/\sqrt{B} (hep-ph/0203056, fig. E.15) ($\times 10^2$)	3.8	-	5.4	-	-	4.8	3.8
S/\sqrt{B} (our estimate) ($\times 10^2$) **	3.7	4.2	4.4	4.5	4.7	4.6	3.1
m [GeV]	250	300	350	400	450	500	
S/\sqrt{B} (ATLAS TDR, fig. 19.62) ($\times 10^2$)	1.9	1.1	0.8	0.7	0.6	0.6	
S/\sqrt{B} (ATLAS TDR, tab. 19.35/36) ($\times 10^2$)	-	1.4	-	-	0.7	-	
S/\sqrt{B} (hep-ph/0203056, fig. E.15) ($\times 10^2$)	2.5	1.6	1.1	0.9	0.8	0.7	
S/\sqrt{B} (our estimate) ($\times 10^2$) **	2.1	1.3	1.0	0.8	0.7	0.6	

Table 5: $gg \rightarrow h \rightarrow ZZ^{(*)} \rightarrow 4l, ll\nu\nu$

m [GeV]	80	100	120	130	140	145	150	160	165	170	180	190
S/\sqrt{B} (CMS Note 1997/057, fig. 1)	0	2.7	5.7	11.0	24.3	27.6	26.0	6.7	5.7	6.3	18.0	24.7
S/\sqrt{B} (CMS 100 fb $^{-1}$ [4]) **	-	2.7	5.3	13.2	22.1	-	27.8	9.4	-	5.5	20.7	25.1
m [GeV]	200	250	275	300	350	400	500	600	700	800	1000	
S/\sqrt{B} (CMS Note 1997/057, fig. 1)	24.3	21.0	-	21.4	23.0	21.0	15.6	-	6.7	-	2.0	
S/\sqrt{B} (CMS 100 fb $^{-1}$ [4]) **	26.1	21.6	17.6	-	22.7	21.6	21.5	17.1	13.6	11.1	9.3	

Table 6: $gg \rightarrow h \rightarrow WW^{(*)} \rightarrow ll\nu\nu, l\nu jj$

m [GeV]	120	130	140	150	160	170	180	190
S/\sqrt{B} (CMS Note 1997/057, fig. 1)	-	-	-	-	27.6	39.4	37.0	14.0
S/\sqrt{B} (CMS Note 1997/083, tab. 1)	7.8	13.7	26.6	32.1	66.3	51.9	34.7	-
S/\sqrt{B} (CMS 100 fb ⁻¹ [4]) **	5.1	9.8	17.8	21.9	47.0	34.4	24.1	19.5
m [GeV]	200	225	250	300	400	500	600	800
S/\sqrt{B} (CMS Note 1997/057, fig. 1)	-	-	-	-	-	-	-	-
S/\sqrt{B} (CMS Note 1997/083, tab. 1)	24.3	16.7	12.5	7.8	10.8	6.2	-	-
S/\sqrt{B} (CMS 100 fb ⁻¹ [4]) **	16.9	-	7.9	19.4	-	-	14.2	11.3

Table 7: $WW \rightarrow h \rightarrow \tau\tau$

m [GeV]	95	100	105	110	115	120	125	130	135	140	145
S/\sqrt{B} (hep-ph/0002036, tab. 5 @ 100fb ⁻¹)	5.0	8.5	10.4	12.4	14.5	16.7	16.4	16.0	13.5	10.8	8.1
S/\sqrt{B} (hep-ph/0203056, p. 64-65 @ 100 fb ⁻¹)	-	-	-	-	12.8	-	15	-	12.1	-	7.6
S/\sqrt{B} (ATL-PHYS-2003-005 [7] @ 100 fb ⁻¹) **	-	-	-	6.7	-	10.4	-	10.4	-	8.7	-

Table 8: $WW \rightarrow h \rightarrow WW$

m [GeV]	105	110	115	120	125	130	135	140
S/\sqrt{B} (hep-ph/0002036, tab. 6 @ 100 fb^{-1})	-	-	-	8.2	-	18.6	-	30.5
S/\sqrt{B} (hep-ph/0203123, tab. 1 @ 100 fb^{-1})	0	5.6	9.7	15.9	24.4	32.8	41.4	50.0
S/\sqrt{B} (hep-ph/0203056, p. 62 @ 100 fb^{-1})	-	-	-	4	-	10.5	-	18.1
S/\sqrt{B} (ATL-PHYS-2003-005(007) [7] @ 100 fb^{-1}) **	-	2.5	(5.6)	6.6 (9.7)	15.7	13.9 (20.5)	-	18.6
m [GeV]	150	155	160	165	170	175	180	185
S/\sqrt{B} (hep-ph/0002036, tab. 6 @ 100 fb^{-1})	43.7	-	66.6	-	59.8	-	47.8	-
S/\sqrt{B} (hep-ph/0203123, tab. 1 @ 100 fb^{-1})	43.6	55.1	66.6	63.2	59.8	53.8	47.8	40.2
S/\sqrt{B} (hep-ph/0203056, p. 62 @ 100 fb^{-1})	29.0	-	45.1	-	42.4	-	33.5	-
S/\sqrt{B} (ATL-PHYS-2003-005(007) [7] @ 100 fb^{-1}) **	26.5	-	34.8	-	34.8	-	27.8	-

References

- [1] This is from Kinnunen's private communication.
- [2] We got to gg only using gg/sum ratios from Lassila's email.
- [3] The results outside the 100 to 130 interval are from Drollinger email.
- [4] The CMS 30 and 100 fb^{-1} results come from CMS CR 2002/020 and private communication respectively (person responsible: R. Kinnunen). They include Kfactors in the background but not in the signal.
- [5] The ATLAS 30 and 100 fb^{-1} results come from the TDR except for VBF which come from ATL-PHYS-2003-005.
- [6] These results are obtained from the line above (which includes $BR(h \rightarrow b\bar{b})$) by dividing out by $BR(h \rightarrow b\bar{b})$. In Drollinger email of May 29, 2003, he cautions that we should not naively scale the 30fb^{-1} results up to $L = 100\text{fb}^{-1}$ using \sqrt{L} scaling (as we have done) since some backoff in b -tagging efficiency ... will be inevitable.
- [7] The ATL-PHYS-2003 is the same as SN-ATLAS-2003-024 and has been confirmed by E. Richter-Was as being the latest with $Kb = Ks = 1$. The numbers in parentheses for channel 8) come from ATL-PHYS-2003-007 where a neural network analysis was performed on the 115-130 GeV mass range.

No Higgs-to-Higgs Parameter Space

- In the original study at Snowmass96, we found many points for which the LHC saw no Higgs signal, even for parameter space regions where none of the decays

$$\begin{aligned} & i) h \rightarrow h'h' , \quad ii) h \rightarrow aa , \quad iii) h \rightarrow h^\pm h^\mp , \quad iv) h \rightarrow aZ , \\ & v) h \rightarrow h^\pm W^\mp , \quad vi) a' \rightarrow ha , \quad vii) a \rightarrow hZ , \quad viii) a \rightarrow h^\pm W^\mp . \end{aligned}$$

was kinematically allowed.

- Things have changed substantially since then.

In particular, the $t\bar{t}h \rightarrow t\bar{t}b\bar{b}$ and $WW \rightarrow h \rightarrow \tau^+\tau^-, WW^*$ modes are looking quite robust, and this makes a big difference.

For all of parameter space such that i)–viii) are forbidden, we have at least one 5σ level signal, typically at least two. Our very worst point (of 1 billion scanned) is illustrated below.

The most difficult point for modes 1)--6):

lambda: 0.0733
kappa: 0.0454
tan(beta): 4.67
mu: 113.
A1: -37.
Ak: -124.

The most visible process at this point:

Higgs No.: 2 Channel No.: 3
Statistical significance: 5.27

mh1: 99.
CV(1): -0.50
Ct(1): -0.47
Cb(1): -1.08
Rglgl(1): 0.20
BRgg(1): 0.24
BRbb(1): 1.08
BRVV(1): 0.23

mh2: 113.
CV(2): -0.71
Ct(2): -0.60
Cb(2): -3.11
Rglgl(2): 0.30
BRgg(2): 0.07
BRbb(2): 1.17
BRVV(2): 0.06

mh3: 152.
CV(3): -0.50
Ct(3): -0.68

Cb(3): 3.46
Rglgl(3): 0.85
BRgg(3): 0.09
BRbb(3): 5.54
BRVV(3): 0.12

ma1: 138.
Ct(4): 0.20
Cb(4): 4.46
Rglgl(4): 0.06
BRgg(4): 0.00
BRbb(4): 1.27

ma2: 164.
Ct(5): 0.06
Cb(5): 1.36
Rglgl(5): 0.00
BRgg(5): 0.00
BRbb(5): 1.38

mc: 161.

Significances for h1:

1	0.41
2	1.07
3	3.72
4	0.70
5	0.00
6	0.00
7	0.00
8	0.00
S _i =1 to 6	3.96
S _i =1 to 8	3.96

Significances for h2:

1	0.27
2	0.80
3	5.27
4	0.70
5	0.14
6	0.00
7	6.13
8	0.18
S_i=1 to 6	5.39
S_i=1 to 8	8.16

Significances for h3:

1	0.77
2	0.44
3	0.00
4	2.42
5	4.05
6	4.85
7	0.00
8	1.11
S_i=1 to 6	6.82
S_i=1 to 8	6.91

Significances for a1:

1	0.00
2	0.00
3	0.60
4	2.31
S_i=1 to 4	2.38

Significances for a2:

1	0.00
2	0.00
3	0.00
4	2.42

We see that this most difficult point for modes 1)–6) is such that it is also just acceptable for modes 7) and 8).

Of course, the h_3 signals are ok if one accepts the fact that they could be combined.

Allowing for Higgs-to-Higgs Decays

- In order to probe the complementary part of the parameter space, we required that at least one of the decay modes $i) - viii)$ is allowed.
- In our set of randomly scanned points, we selected those for which all the statistical significances in modes 1) – 8) are below 5σ .
- Some remarks:
 1. We obtained a lot of points, all with similar characteristics. Namely, in the Higgs spectrum, we always have a very SM-like CP-even Higgs boson with a mass between 115 and 135 GeV (*i.e.* above the LEP limit), which can be either h_1 or h_2 , with a reduced coupling to the gauge bosons $R_1 \simeq 1$ or $R_2 \simeq 1$, respectively.
 2. This state decays dominantly to a pair of (very) light CP-odd states, $a_1 a_1$, with m_{a_1} between 5 and 65 GeV.
The singlet component of a_1 has to be small in order to have a large $h_1 \rightarrow a_1 a_1$ or $h_2 \rightarrow a_1 a_1$ branching ratio when the h_1 or h_2 , respectively, is the SM-like Higgs boson.

3. Further, when the h_1 or h_2 is very SM-like, one has $R'_{11} \simeq 0$ or $R'_{21} \simeq 0$, respectively, so that the $e^+e^- \rightarrow h_1 a_1$ or $e^+e^- \rightarrow h_2 a_1$ associated production places no constraint on the light CP-odd state at LEP.
4. We have selected six difficult benchmark points, displayed in Table 9.
5. For points 1 – 3, h_1 is the SM-like CP-even state, while for points 4 – 6 it is h_2 .

We have chosen the points so that $h_{1,2}$ and a_1 have different masses.

6. The main characteristics of the benchmark points are displayed in Table 9.
7. Note the large $B(h \rightarrow a_1 a_1)$ of the SM-like h ($h = h_1$ for points 1 – 3 and $h = h_2$ for points 4 – 6).
8. For points 4 – 6, with $m_{h_1} < 100$ GeV, the h_1 is mainly singlet. As a result, R'_{11} is very small, implying no LEP constraints on the h_1 and a_1 from $e^+e^- \rightarrow h_1 a_1$ production.
9. We note that in the case of the points 1 – 3, the h_2 would not be detectable either at the LHC or the LC. For points 4 – 6, the h_1 , though light, is singlet in nature and would not be detectable.
10. Further, the h_3 or a_2 will only be detectable for points 1 – 6 if a super high energy LC is eventually built so that $e^+e^- \rightarrow Z \rightarrow h_3 a_2$ is possible.
11. Thus, we will focus on searching for the SM-like h_1 (h_2) for points 1 – 3 (4 – 6) using the dominant $h_1(h_2) \rightarrow a_1 a_1$ decay mode.
12. In the case of points 2 and 6, it should be noted that the $a_1 \rightarrow \tau^+ \tau^-$

decays are dominant, with $a_1 \rightarrow jj$ decays making up most of the rest. For points 1 and 3 – 5 for which $B(a_1 \rightarrow b\bar{b})$ is substantial, the b jets will not be that energetic and tagging will be somewhat inefficient. Thus, we have chosen not to implement b -tagging as part of the experimental procedures detailed next.

Point Number	1	2	3	4	5	6
Bare Parameters						
λ	0.2872	0.2124	0.3373	0.3340	0.4744	0.5212
κ	0.5332	0.5647	0.5204	0.0574	0.0844	0.0010
$\tan \beta$	2.5	3.5	5.5	2.5	2.5	2.5
μ_{eff} (GeV)	200	200	200	200	200	200
A_λ (GeV)	100	0	50	500	500	500
A_κ (GeV)	0	0	0	0	0	0
CP-even Higgs Boson Masses and Couplings						
m_{h_1} (GeV)	115	119	123	76	85	51
R_1	1.00	1.00	-1.00	0.08	0.10	-0.25
t_1	0.99	1.00	-1.00	0.05	0.06	-0.29
b_1	1.06	1.05	-1.03	0.27	0.37	0.01
Relative gg Production Rate	0.97	0.99	0.99	0.00	0.01	0.08
$B(h_1 \rightarrow b\bar{b})$	0.02	0.01	0.01	0.91	0.91	0.00
$B(h_1 \rightarrow \tau^+\tau^-)$	0.00	0.00	0.00	0.08	0.08	0.00
$B(h_1 \rightarrow a_1 a_1)$	0.98	0.99	0.98	0.00	0.00	1.00
m_{h_2} (GeV)	516	626	594	118	124	130
R_2	-0.03	-0.01	0.01	-1.00	-0.99	-0.97
t_2	-0.43	-0.30	-0.10	-0.99	-0.99	-0.95
b_2	2.46	-3.48	3.44	-1.03	-1.00	-1.07
Relative gg Production Rate	0.18	0.09	0.01	0.98	0.99	0.90
$B(h_2 \rightarrow b\bar{b})$	0.01	0.04	0.04	0.02	0.01	0.00
$B(h_2 \rightarrow \tau^+\tau^-)$	0.00	0.01	0.00	0.00	0.00	0.00
$B(h_2 \rightarrow a_1 a_1)$	0.04	0.02	0.83	0.97	0.98	0.96
m_{h_3} (GeV)	745	1064	653	553	554	535

Point Number	1	2	3	4	5	6
CP-odd Higgs Boson Masses and Couplings						
m_{a_1} (GeV)	56	7	35	41	59	7
t'_1	0.05	0.03	0.01	-0.03	-0.05	-0.06
b'_1	0.29	0.34	0.44	-0.20	-0.29	-0.39
Relative gg Production Rate	0.01	0.03	0.05	0.01	0.01	0.05
$B(a_1 \rightarrow b\bar{b})$	0.92	0.00	0.93	0.92	0.92	0.00
$B(a_1 \rightarrow \tau^+\tau^-)$	0.08	0.94	0.07	0.07	0.08	0.90
<hr/>						
m_{a_2} (GeV)	528	639	643	560	563	547
Charged Higgs Mass (GeV)	528	640	643	561	559	539
<hr/>						
Most Visible Process No.	2 (h_1)	2 (h_1)	8 (h_1)	2 (h_2)	8 (h_2)	8 (h_2)
Significance at 300 fb ⁻¹	0.48	0.26	0.55	0.62	0.53	0.16

Table 9: In the table, we give properties of selected scenarios that could escape detection at the LHC. In the table, R_i , t_i and b_i are the ratios of the h_i couplings to VV , $t\bar{t}$ and $b\bar{b}$, respectively, as compared to those of a SM Higgs boson with the same mass; t'_1 and b'_1 denote the magnitude of the $i\gamma_5$ couplings of a_1 to $t\bar{t}$ and $b\bar{b}$ normalized relative to the magnitude of the $t\bar{t}$ and $b\bar{b}$ SM Higgs couplings. We also give the production for $gg \rightarrow h_i$ fusion relative to the gg fusion rate for a SM Higgs boson with the same mass. Important absolute branching ratios are displayed. For points 2 and 6, $B(a_1 \rightarrow jj) \simeq 1 - B(a_1 \rightarrow \tau^+\tau^-)$. For the heavy h_3 and a_2 , we give only their masses. In the case of the points 2 and 6, decays of a_1 into light quarks start to contribute. For all points 1 – 6, the statistical significances for the detection of any Higgs boson in any of the channels 1) – 8) (as listed in the introduction) are tiny; their maximum is indicated in the last row, together with the process number and the corresponding Higgs state.

Simulations and LHC/LC Complementarity

- As we have already stressed, for the points summarized in Table 9 the a_1 is light and decays almost entirely into $b\bar{b}$ (or jj for points 2 and 6)¹ and $\tau^+\tau^-$.

The possible final states are thus $b\bar{b}b\bar{b}$, $b\bar{b}\tau^+\tau^-$ and $\tau^+\tau^-\tau^+\tau^-$ or $b \rightarrow j$ analogues.

1. A $4b$ -signal would be burdened by a large QCD background even after implementing b -tagging.
2. A $4j$ -signal would be completely swamped by QCD background.
3. Meanwhile, the 4τ -channel would not allow one to reconstruct the h_1, h_2 resonances.
4. Hence, we will focus in this study on the $2b2\tau$ or $2j2\tau$ signature.
5. In addition, we will be looking at τ 's decaying leptonically to electrons and muons, yielding some amount of missing (transverse) momentum, p_{miss}^T , that could be projected onto the visible e, μ -momenta in an attempt to reconstruct the parent τ -direction.

¹In the following discussions, there are many places where $b\bar{b}$ should be replaced by jj for points 2 and 6, where j refers to any possible non- b jet. In any case, the analysis does not employ b -tagging.

6. Since for points 2 and 6 the a_1 does not decay to $b\bar{b}$ and since the b and \bar{b} that do come from a_1 are not very energetic given the modest m_{a_1} mass for points 1 and 3 – 5, we will not employ b -tagging as part of our analysis.

- Results for the LHC

- As stated earlier, we expect that $WW \rightarrow h \rightarrow aa$ allows the best hope for Higgs detection in these difficult NMSSM cases.

(We reemphasize that the h_1 [cases 1 – 3] or h_2 [cases 4 – 6] has nearly full SM strength coupling to WW .)

- However, the $b\bar{b}\tau^+\tau^-$ final state of relevance is complex and subject to large backgrounds. and the a_1 masses of interest are very modest in size.

- In order to extract the $2b2\tau$ NMSSM Higgs boson signature from the central detector region, we have exploited forward and backward jet tagging on the light quarks emerging after the double W -strahlung preceding WW -fusion.

If we require two forward/backward jets, it is clear that the leading background is due to $t\bar{t}$ production (since we are assuming a heavy SUSY

spectrum) and decay via the purely SM process, $gg \rightarrow t\bar{t} \rightarrow b\bar{b}W^+W^- \rightarrow b\bar{b}\tau^+\tau^- + p_{\text{miss}}^T$, in association with forward and backward jet radiation.

- Thus, at the LHC, the signature is
 - 2 forward/backward jets, at least 2 central jets, p_{miss}^T and a $\tau^+\tau^-$ pair decaying leptonically (to electrons and/or muons).
- In order to carry out realistic numerical simulations, we have used a modification of the MSSM implementation of the HERWIG event generator in conjunction with the GETJET code for calorimeter emulation and jet reconstruction. An ISAWIG format input file has been edited by hand to incorporate the Higgs boson mass spectrum and decay rates as predicted for each of the NMSSM points 1 – 6, while in the main HERWIG code (v6.4) the subroutine implementing the vector-vector fusion process has been modified to account for the different Higgs- VV vertices pertaining to the NMSSM points 1 – 6 given in Table 9.

The above codes do not include K factors for either the signal or the background.

- An outline of the selection procedure and cuts used is the following.

- Acceptance cuts:

$$|\eta_{\text{jet}}| < 5, \quad p_{\text{jet}}^T > 20 \text{ GeV}, \quad \Delta R_{\text{jet-jet}} > 0.7,$$

$$\eta_{\text{jet}}^{\text{max}} \cdot \eta_{\text{jet}}^{\text{min}} < 0, \quad |\eta_{\text{lepton}}| < 2.5,$$

$$p_{\text{lepton}}^T > 10 \text{ GeV}, \quad \text{no lepton isolation.}$$

- Since the a_1 will not have been detected previously, we must assume a value for m_{a_1} . It will be necessary to repeat the analysis for densely spaced m_{a_1} values and look for the m_{a_1} choice that produces the best signal.
- We look among the central jets for the combination with invariant mass M_{jj} closest to m_{a_1} (no b -tagging is enforced, b 's are identified as non-forward/backward jets).
- Select the two highest transverse-momentum leptons in any flavor combination and with opposite charge. After ensuring that these are not back-to-back (by requiring that their relative angle is smaller than 175 degrees), resolve the p_{miss}^T along their directions and reconstruct the invariant mass, $M_{\tau^+\tau^-}$.
- Plot the $M_{jj\tau^+\tau^-}$ invariant mass using the four four-momenta reconstructed in the two previous steps, as seen in the top plot of Fig. 1 — the plot presented assumes that we have hit on the correct m_{a_1} choice.

LHC, $\sqrt{s_{pp}} = 14$ TeV

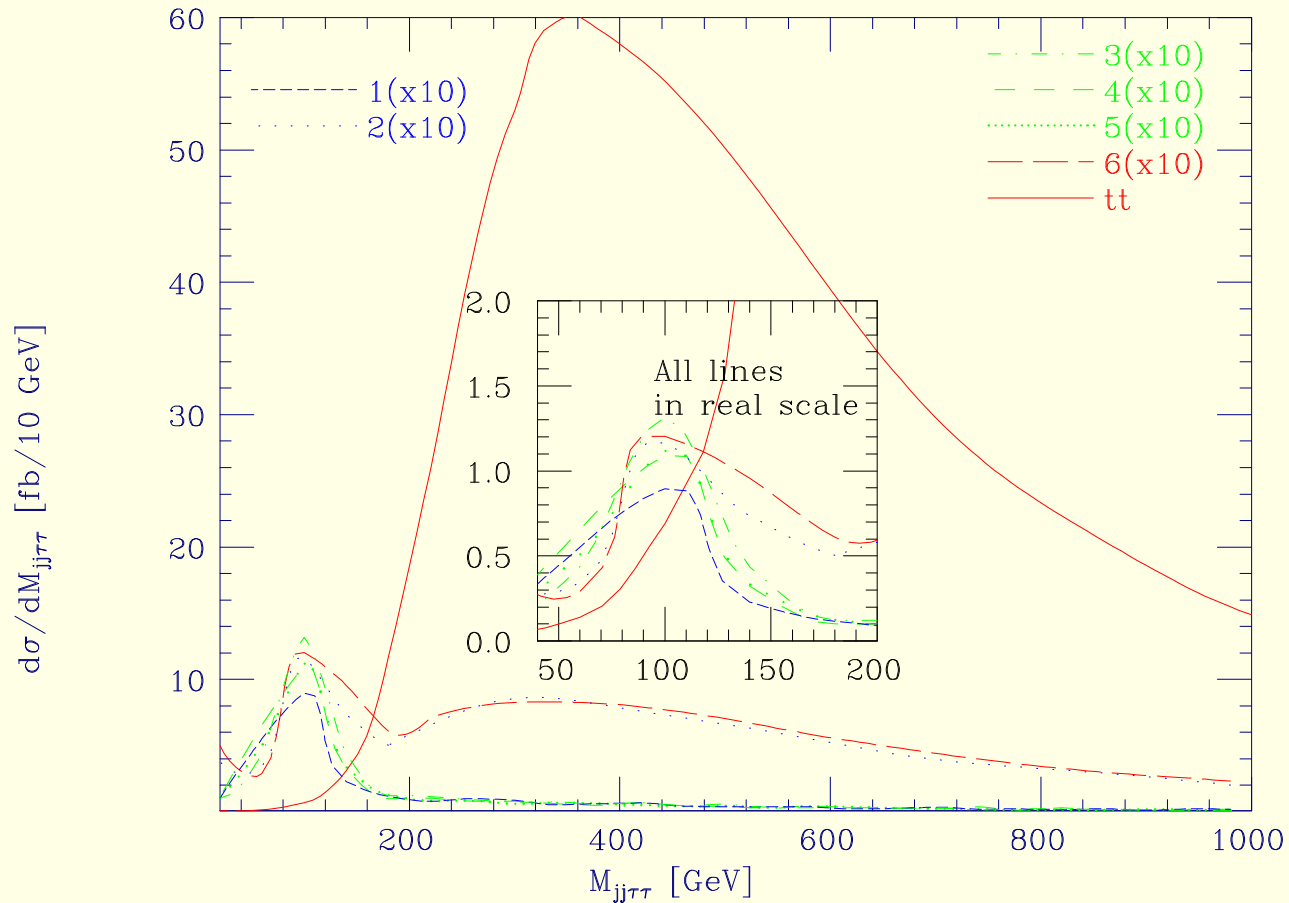


Figure 1: Reconstructed mass of the $jj\tau^+\tau^-$ system for signals and backgrounds after the selections described, at the LHC. We plot $d\sigma/dM_{jj\tau^+\tau^-}$ [fb/10 GeV] vs $M_{jj\tau^+\tau^-}$ [GeV]. The lines corresponding to points 4 and 5 are visually indistinguishable. No \mathbf{K} factors are included.

- **Remarks:**

1. For all six NMSSM setups, the Higgs resonance produces a bump in the very end of the low mass tail of the $t\bar{t}$ background (see the insert in the top frame of Fig. 1).
2. However, after summing the background distribution and any one of the signal spectra, it could be difficult to ascertain the existence of the h_1 or h_2 peaks from the net line shapes.
3. Still, statistics are significant.

To estimate S/\sqrt{B} , we assume $L = 300 \text{ fb}^{-1}$, a K factor of 1.1 for WW fusion and a K factor of 1.6 for the $t\bar{t}$ background.

(These K factors are not included in the plots of Fig. 1.)

We sum events over the region $60 \leq M_{jj\tau^+\tau^-} \leq 90 \text{ GeV}$. For points 1 – 6 we obtain signal rates of about $S = 890, 600, 750, 1030, 915, 500$, respectively.

The $t\bar{t}$ background rate is $B \sim 320$.

This gives $N_{SD} = S/\sqrt{B}$ of 50, 34, 42, 58, 51, 28 for points 1 – 6, respectively. These are substantial.

However, given the broad distribution of the signal, it is clear that the crucial question will be the accuracy with which the background shape can be predicted from theory.

The background *normalization* after the cuts imposed in our analysis would be very well known from the higher $M_{jj\tau^+\tau^-}$ regions.

- **The LC scenario**

- While further examination of and refinements in the LHC analysis may ultimately lead us to have good confidence in the viability of the NMSSM Higgs boson signals discussed above, an enhancement at low $M_{jj\tau^+\tau^-}$ of the type shown (for some choice of m_{a_1}) will nonetheless be the only evidence on which a claim of LHC observation of Higgs bosons can be based.

Ultimately, a means of confirmation and further study will be critical.

Thus, it is important to summarize the prospects at the LC, with energy up to 800 GeV, in the context of the difficult scenarios 1 — 6 of Table 9 discussed here.

In the following, $h = h_1$ for points 1–3 and $h = h_2$ for points 4–6 in Table 9.

- Because the ZZh coupling is nearly full strength in all cases, and because the h mass is of order 100 GeV, discovery of the h will be very straightforward via $e^+e^- \rightarrow Zh$ using the $e^+e^- \rightarrow ZX$ reconstructed

M_X technique which is independent of the “unexpected” complexity of the h decay to $a_1 a_1$.

This will immediately provide a direct measurement of the ZZh coupling with very small error.

The next stage will be to look at rates for the various h decay final states, F , and extract $BR(h \rightarrow F) = \sigma(e^+e^- \rightarrow Zh \rightarrow ZF) / \sigma(e^+e^- \rightarrow Zh)$.

For the NMSSM points considered here, the main channels would be $F = b\bar{b}b\bar{b}$, $F = b\bar{b}\tau^+\tau^-$ and $F = \tau^+\tau^-\tau^+\tau^-$.

At the LC, a fairly accurate determination of $BR(h \rightarrow F)$ should be possible in all three cases. This would allow us to determine $BR(h \rightarrow a_1 a_1)$ independently.

- Here, we consider the equally (or perhaps more) useful vector-vector fusion mode that will be active at a LC.
 1. At 800 GeV or above, it is the dominant Higgs boson production channel for CP-even Higgs bosons in the intermediate mass range.
 2. Contrary to the case of the LHC though, the dominant contribution (from WW fusion) does not allow for forward and backward particle tagging,

as the incoming electron and positron convert into (anti)neutrinos, which escape detection.

3. Although the ZZ fusion contribution would allow tagging of forward/backward e^- and e^+ , the cross section is a factor of 10 smaller in comparison.
 4. At the LC, the ZZ background plays a significant role and has been simulated in our HERWIG and (LC-adjusted) GETJET numerical analysis.
- At a LC, the optimal signature will thus be different than at the LHC and a different set of selection criteria are needed. We choose selection criteria that will retain both the WW and the ZZ fusion Higgs boson production processes.
 - We require an even number of oppositely-charged leptons ($n_\ell = 2, 4, \dots$).
 - If $n_\ell \geq 4$ then we demand that two of these must be an electron and a positron, so that the final state would be consistent with having been generated by forward/backward e^\pm tagging in ZZ -fusion and $\tau^+\tau^-$ decays in which both τ 's decay leptonically (to electron and muons).
 - Finally, we require at least 2 central jets and significant p_{miss}^T .

Given the required final state as above, we employ the following selection procedure and cuts.

- Acceptance cuts:

$$\begin{aligned}
 |\cos \theta_{\text{jet}}| &< 0.990, & p_{\text{jet}}^T &> 5 \text{ GeV}, & \Delta R_{\text{jet-jet}} &> 0.4, \\
 \eta_{e^+}^{\text{max}} \cdot \eta_{e^-}^{\text{min}} &< 0 \text{ (if } n_\ell \geq 4), & |\cos \theta_{\text{lepton}}| &< 0.995, \\
 p_{\text{lepton}}^T &> 5 \text{ GeV}, & & \text{no lepton isolation.}
 \end{aligned}$$

- We look among the central jets for the combination with invariant mass M_{jj} closest to m_{a_1} (again, no b -tagging is enforced — b 's are identified as non-forward/backward jets).

- Out of the n_ℓ leptons, upon excluding the e^+e^- pair in which the electron and positron are those with the largest rapidities if $n_\ell \geq 4$, select the two with highest transverse-momenta in any flavor combination and with opposite charge.
After ensuring that these are not back-to-back, resolve the p_{miss}^T along their directions and reconstruct the invariant mass $M_{\tau^+\tau^-}$.
- Plot the $M_{jj\tau^+\tau^-}$ invariant mass (see the bottom of Fig. 2) using the four four-momenta reconstructed in the two previous steps.

Note that it is not fruitful to place cuts on the invariant masses M_{jj} and $M_{\tau^+\tau^-}$ that exclude $M_{jj}, M_{\tau^+\tau^-} \sim m_Z$ in an attempt to reduce the ZZ background.

This is because the SM-like h mass is typically of order 115 GeV, *i.e.* not so far from m_Z , and the experimental resolutions in the two masses M_{jj} and $M_{\tau^+\tau^-}$ are poor, either because of the large number of hadronic tracks or the missing longitudinal momenta of the (anti) neutrinos, respectively.

- Finally notice that we have included Initial State Radiation (ISR) and beam-strahlung effects, as predicted using the HERWIG default. These tend to introduce an additional unresolvable missing longitudinal momentum, although to a much smaller extent than do the Parton Distribution Functions (PDFs) in hadron-hadron scattering at the LHC.

LC, $\sqrt{s_{e^+e^-}} = 800 \text{ GeV}$

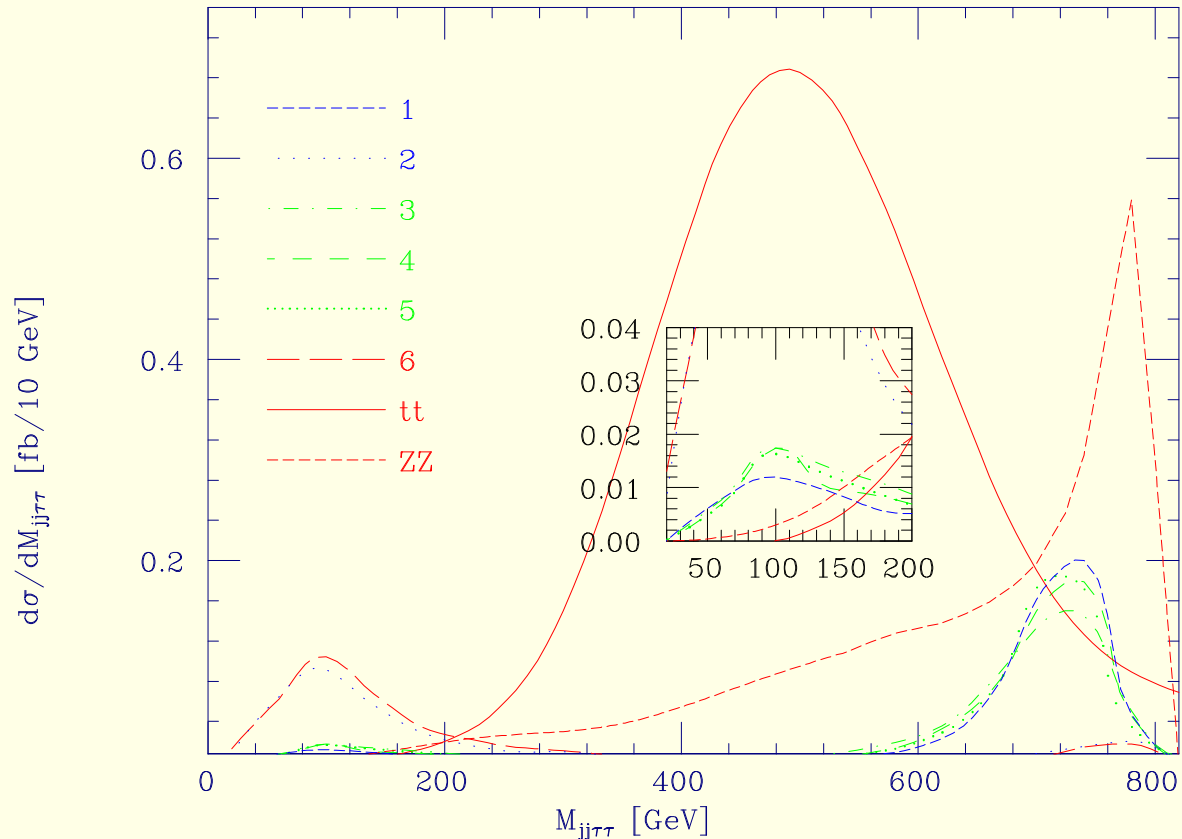


Figure 2: *As above, except at the LC.*

● **Remarks:**

1. From Fig. 2, we see that the $M_{jj\tau^+\tau^-}$ distribution reconstructed at the LC displays resonance mass peaks (again centered at 100 GeV) for the

SM-like h_1 (points 1 – 3) or h_2 (points 4 – 6) that are very clearly visible above both the $t\bar{t}$ and ZZ backgrounds, particularly for the case of points 2 and 6 (see insert in the bottom frame of Fig. 2).

2. Assuming $L = 500 \text{ fb}^{-1}$, the points 1,3,4,5 yield 5 events per 10 GeV bin, on average, in the 50 to 150 GeV mass interval of interest. (The signals for points 2 and 6 are still larger.)

This would constitute a convincing signal given the very small size predicted for the background.

3. Notice that, although to assign the entire missing transverse momentum to the τ -lepton system may seem not entirely appropriate (given the forward/backward (anti)neutrinos from the incoming electrons and positrons in WW fusion), this does not hamper the ability to reconstruct the Higgs mass peaks. However, there will be a proportion of the signal events that tend to reproduce the overall $\sqrt{s_{e^+e^-}}$ value in the $M_{jj\tau^+\tau^-}$ distribution.

The effect is more pronounced for points 1 and 3–5, which is where the a_1 mass is larger (see Table 9) so that most of the hadronic tracks composing the emerging jets easily enter the detector region.

For points 2 and 6, where m_{a_1} is below 10 GeV, this may often not be true and it appears that the consequent effect of these hadrons escaping detection is that of counterbalancing the p_{miss}^T contributions related to the neutrinos left behind in WW fusion reactions.

For the case of the ZZ noise, in the limit of full coverage and perfect resolution of the detector, one would have $M_{jj\tau^+\tau^-} \equiv \sqrt{s_{e^+e^-}}$, which explains the concentration of events with $M_{jj\tau^+\tau^-}$ around 800 GeV. (The “tails” beyond $\sqrt{s_{e^+e^-}}$ are due to the smearing of the visible tracks in our Monte Carlo analysis.)

Conclusions

- We are really quite close to a no-lose theorem for NMSSM Higgs detection at the LHC.

1. If Higgs-to-Higgs decays are not important then the conventional SM search modes will work, although the signals might not be much better than 5σ with $L = 300\text{fb}^{-1}$ of integrated luminosity.

(I.e. don't give up on the conventional signals after just $L = 30\text{fb}^{-1}$.)

2. We found that the only parameter choices for which the conventional modes do not work are such that the most SM-like of the CP-even Higgs bosons, h , is relatively light and decays primarily to a pair of CP-odd Higgs states, $h \rightarrow aa$.

In this case, there will be a statistically highly significant LHC signal (from $WW \rightarrow h \rightarrow aa$) of an $S/B \sim (500 - 1000)/300$ bump (for $L = 300 \text{ fb}^{-1}$) in the low-mass tail of a rapidly falling $jj\tau^+\tau^-$ mass distribution.

The LHC would thus give a very strong indication of the presence of a Higgs boson even in this case.

3. However, this detection mode is not exactly in the gold-plated category. There will undoubtedly be other possible interpretations for the bump observed.

- Thus, the LC will be absolutely essential in order to confirm that the enhancement seen at the LHC really does correspond to a Higgs boson.

At the LC, discovery of a light SM-like h is guaranteed to be possible in the Zh final state using the recoil mass technique.

Further, we have seen that WW, ZZ fusion production of the h will also produce a viable signal in the $jj\tau^+\tau^-$ final state — and perhaps in the $4j$ and $\tau^+\tau^-\tau^+\tau^-$ final states as well, although we have not examined these (yet).

- As we have stressed, for parameter space points of the type we have discussed here, detection of any of the *other* NMSSM Higgs bosons is likely to be impossible at the LHC and is likely to require an LC with $\sqrt{s_{e^+e^-}}$ above the relevant thresholds for $h'a'$ production, where h' and a' are heavy CP-even and CP-odd Higgs bosons, respectively.
- We must develop means by which one could make a convincing case that

the “hump signal” for the $h \rightarrow aa$ mode really does correspond to a (NMSSM) Higgs boson. Possible steps include:

1. Improved techniques for extracting a signal are likely to be developed once data is in hand and the $t\bar{t}$ background can be more completely modeled.
2. A study (in progress) of the mass resolution in m_{a_1} might reveal good peaking, which would provide solid evidence for the $a_1 a_1$ mode.
3. We should study what the resolution in m_h is.

For the models considered, the range of m_h ($m_h \in [115 \text{ GeV}, 130 \text{ GeV}]$) is not very large.

We would want to know that we could distinguish such a range from, say, $m_h = 150 \text{ GeV}$ which is beyond the NMSSM (when perturbatively constrained up to M_U) limit for a very SM-like h .

4. A very important thing would be to establish the signal in the $4b$ final state in addition to the $2b2\tau$ final state studied so far.

If these two channels are in the ratio expected for an a -type Higgs boson that couples to mass, that would be a very strong argument in favor of the Higgs interpretation.

All these steps would help greatly to convince us that an observation of this type of “hump signal” really does correspond to an NMSSM Higgs boson.

- Clearly, if SUSY is discovered and no Higgs bosons are detected in the standard MSSM modes, a careful search for the signal we have considered should have a high priority.
- We should remark that the $h \rightarrow aa$ search channel considered here in the NMSSM framework is also highly relevant for a general two-Higgs-doublet model, 2HDM.

It is really quite possible that the most SM-like CP-even Higgs boson of a 2HDM will decay primarily to two CP-odd states. This is possible even if the CP-even state is quite heavy, a situation that does not arise in the NMSSM.

- In a similar vein, one needs to keep in mind the fact that an MSSM Higgs sector with one-loop induced CP violation might be such as to necessitate detection of a $h \rightarrow aa$ type signal in order to discover a Higgs boson at the LHC.
- Finally, we will have to address the one possible remaining hole in our NMSSM LHC “no-lose” theorem (other than SUSY decays, which are now being looked at by us), namely a CP-violating NMSSM Higgs sector with **five** mixed Higgs.